

Exfoliation and Stability Studies of Germanane and its Derivatives

Research Thesis

Presented in Partial Fulfillment of the Requirements for graduation

“with Research Distinction in Chemistry” in the undergraduate colleges of The Ohio State  
University

By

Fan Fan

The Ohio State University

November 2014

Thesis Committee:

Joshua Goldberger, Project Advisor

Yiying Wu

## Abstract

The discovery of graphene has demonstrated that stable single-layer sheets can be isolated from the bulk materials. In the previous work, we have successfully isolated single-layer hydrogen-terminated-germanium (germanane, GeH) sheets which have unique electronic properties distinct from the bulk materials. In order to understand the doping effect of GeH, we have synthesized phosphorus-doped germanane (P-GeH), gallium-doped germanane (Ga-GeH) and arsenic-doped germanane (As-GeH) via the topochemical deintercalation of CaGeP, CaGeGa and CaGeAs, respectively. Similar to GeH, the doped GeH crystals can also be exfoliated into single- and few-layer sheets on SiO<sub>2</sub>/Si substrates mechanically. The optimized tape for exfoliating GeH crystals into measurable multilayer flakes is polydimethylsiloxane (PDMS). Lithium phenylacetylide can be used to clean PDMS residues left on the flakes. All the four van der Waals materials can be oxidized in the air at different oxidizing rates but the oxidization is limited to the surface layers based on the X-ray photoelectron spectroscopy data and atomic force microscopy (AFM) images. In addition, the oxidized layers are dissolvable in the HCl aqueous solution while the fresh layers are still resistant to the HCl aqueous solution.

## Acknowledgments

First of all, I would express my sincerest gratitude to my thesis advisor, Prof. Joshua Goldberger and thank you so much for offering a research opportunity, constant support and patient guidance on my thesis. Thank you to Basant Chitara for your suggestions at the beginning of my thesis. I would also like to thank Nick Cultrara and Shishi Jiang for preparing outstanding crystal samples and suggestions to my work. Finally, I would like to extend a special gratitude to my parents for their endless support in the past two and half years.

## Vita

### Education

2012.....Heilongjiang University, Heilongjiang Province, China

2014..... B.S., Chemistry with ASC certification

### Field of Study

Major Field: Chemistry

## Table of Contents

Abstract .....	i
Acknowledgements .....	ii
Vita .....	iii
List of Figures .....	v
Chapter 1: Introduction .....	1
Chapter 2: Optimized Exfoliation of Multilayers	
2.1: Exfoliation and Characterization .....	4
2.2: Optimized Tape Choice for Exfoliation .....	8
2.3: Optimized Cleaning Process .....	10
Chapter 3: Synthesis and Characterization of Germanane and its Derivatives .....	12
Chapter 4: Stability Studies	
4.1: Air-Stability (XPS) .....	15
4.2: Air-Stability (AFM) .....	16
4.3: HCl-Stability .....	19
Chapter 5: Further Work .....	22
Conclusion .....	24
References .....	25

## List of Figures

Figure 2.1. Optical micrograph of SiO <sub>2</sub> /Si wafer and applied substrate (right corner) .....	4
Figure 2.2. (a) AFM image (top), optical image (inset) and height profile of few-layer GeH flake on SiO <sub>2</sub> /Si. (b) AFM image (top), optical image (inset) and height profile of single-atom-thick GeH flake .....	5
Figure 2.3. (a) AFM image (top), height profile (bottom), and optical micrograph (inset) of 9.85-nm-thick P-GeH sheet. (b) AFM image (top), height profile (bottom), and optical micrograph (inset) of 9.1-nm-thick P-GeH sheet .....	6
Figure 2.4. (a) AFM image (top), height profile (bottom), and optical micrograph (inset) of 14-nm-thick P-GeH sheet. (b) AFM image (top), height profile (bottom), and optical micrograph (inset) of 14.3-nm-thick P-GeH sheet .....	6
Figure 2.5. (a) AFM image (top), height profile (bottom), and optical micrograph (inset) of 23.6-nm-thick P-GeH sheet. (b) AFM image (top), height profile (bottom), and optical micrograph (inset) of 36.2-nm-thick Ga-GeH sheet .....	7
Figure 2.6. AFM image (top), height profile (bottom), and optical micrograph (inset) of 115.4-nm-thick GeH sheet .....	7
Figure 2.7. Diagrammatic sketch of atomic force microscopy (AFM) structure .....	8
Figure 2.8. (a) Optical image of scotch tape. (b) Optical image of polydimethylsiloxane (PDMS). (c) Optical image of Kapton tape .....	9
Figure 2.9. (a) Optical image of spin-coat comparison test sample. The left 4 substrates were exfoliated by the scotch tape while the right 4 were exfoliated by kapton tape. (b) AFM image (top), height profile (bottom), and optical micrograph (inset) of a scotch tape exfoliated As-GeH sample. (c) AFM image (top), height profile (bottom), and optical micrograph (inset) of a PDMS exfoliated Ga-GeH sample .....	10
Figure 2.10. (a) Fresh exfoliated Ga-GeH flake. (b) The same flake after 90 min lithium phenylacetylide treatment. (c) Height profile of (a) and (b) .....	11
Figure 2.11. Schematic illustration of PDMS dissolving in lithium phenylacetylide .....	11
Figure 3.1 (a) Schematic illustration of the GeH preparation. 9b) Optical image of CaGe <sub>2</sub> crystal. (c) Optical image of GeH crystal. (d) XRD diagram of (b). (e) XRD diagram of GeH .....	12
Figure 3.2. Schematic diagrams of (a) As-GeH and P-GeH and (b) Ga-GeH .....	13
Figure 3.3. (a) XRD spectra (b) FTIR spectra and (c) Raman spectra of Ga-GeH, As-GeH and GeH .....	14
Figure 4.1. (a) 2p XPS spectra of Ga-GeH and (b) 2p XPS spectra of As-GeH .....	16

Figure 4.2. Time-dependent XPS spectra of GeH after exposure to the air for a period of time .....	16
Figure 4.3. (a) AFM image of a fresh Ga-GeH flake. (b) AFM image of (a) after one week in air. (c) AFM image of (b) after 30 seconds 1 M HCl treat. (d) Height profile of (a), (b) and (c). (e) AFM of another fresh Ga-GeH flake. (f) AFM of (e) after 30 seconds in 1 M HCl. (g) Height profile of (e) and (f) .....	17
Figure 4.4. (a) AFM image of a fresh As-GeH flake. (b) AFM image of (a) after one week in air. (c) Height profile of (a) and (b). (d) AFM of another fresh As-GeH flake. (e) AFM of (d) after 30 seconds in 1 M HCl. (f) Height profile of (d) and (e) .....	17
Figure 4.5. a) AFM image of a fresh P-GeH flake. (b) AFM image of (a) after one week in air. (c) Height profile of (a) and (b). (d) AFM of another fresh P-GeH flake. (e) AFM of (d) after 30 seconds in 1 M HCl. (f) Height profile of (d) and (e) .....	18
Figure 4.6. a) AFM image of a fresh GeH flake. (b) AFM image of (a) after one week in air. (c) Height profile of (a) and (b). (d) AFM of another fresh GeH flake. (e) AFM of (d) after 30 seconds in 1 M HCl. (f) Height profile of (d) and (e) .....	19
Figure 4.7. (a) AFM image of fresh-exfoliated Ga-GeH. (b) AFM image of (a) after 30 seconds 1 M HCl treatment. (c) AFM image of (b) after 1200 seconds 1 M HCl treatment. (d) Height profile of (a), (b) and (c) .....	20
Figure 5. (a) AFM image of fresh Ga-GeH flake. (b) AFM of (a) after 30 second oxygen plasma followed by 30 seconds 1 M HCl treatment. (c) Height profile of (a) and (b). (d) AFM of fresh Ga-GeH flake. (e) AFM of (d) after 30 seconds UV-ozone plasma followed by 30 seconds 1 M HCl. (f) Height profile of (d) and (e) .....	23

## Chapter 1: Introduction

The discovery of stable single-atom-thick graphene has demonstrated that it is possible to isolate stable single-layer-thick materials from the bulk materials whose crystal structures are mainly bonded by weak van der Waals interactions.<sup>1</sup> Single-layer materials have unique electric properties distinct from their parent materials, which makes them promising candidates in potential applications such as sensors, transistors and LED.<sup>2-5</sup> Graphene's success motivates the exploration of properties and stabilities of other single-layer 2D materials. For example, MoS<sub>2</sub> crystals have a 1.29 eV indirect band gap while its single-layer sheets have a direct band gap at 1.8 eV, which reveals the potential application as high mobility transistors for isolated MoS<sub>2</sub> single layers.<sup>6-8</sup>

As for 2D materials, their bonding strength on the 2D direction is much stronger than it is on a third dimension. Besides, it has been demonstrated that most bulk semiconductor materials from II-VI groups can be dimensionally reduced to 2D materials by the solution-phase solvothermal synthesis method accompanying with alkylamine ligands.<sup>9-13</sup> The conventional van der Waals materials are not chemically functionalized, which limits the practical applications. In contrast, the 2D materials would have many optical and electronic applications after adding electrically active layers.<sup>14</sup> This terminal substituent creates a new direction to not only modify the fundamental electric properties of layered materials but also functionalize the layered materials based on the specific sensing applications.<sup>14</sup> For example, graphene has been reported to be grafted with some organic functional groups, terminated with hydrogen and be oxidized.<sup>15,16</sup> However, the original mobility of carriers is undermined after adding the functionalized layer materials and the stability is also eliminated.<sup>17</sup>



It has been demonstrated that the  $\text{GaGe}_2$  can be converted to the hydrogen-terminated germanium crystals in the concentrated HCl aqueous solution.<sup>18</sup> The Ge in GeH crystals is in the  $\text{sp}^3$ -hybridized state which may maintain good conductivity. Recently, Goldberger's group has developed gram-scale crystals of GeH whose single-layer sheet has a calculated 1.53 eV direct band gap and has proven that the surface layer of GeH would be oxidized slowly in the air.<sup>14</sup> In order to study the doping effect on germanane crystals, we plan to develop both n-type and p-type germanane crystals to tune the optical and electric properties of GeH for practical applications.<sup>19</sup>

The unique and useful electric properties such as the direct band gap is calculated based on the single-layer sheets. Generally, the weak van der Waals interactions between two adjacent sheets are just 40 meV to  $\sim 70$  meV so single-layer sheets and multilayer sheets can be collected by exfoliation.<sup>19</sup> Mechanical exfoliation which uses tapes such as scotch tape to isolate thin sheets is the most common and powerful exfoliation method because this method does not destroy thin flakes easily compared with other methods including chemical exfoliation and can create large single-atom-thick flakes ( $\sim 10\mu\text{m}$  level) which is convenient for making fabricating devices.<sup>19</sup> We have demonstrated that the pure GeH has being exfoliated into single layer sheets at  $2\mu\text{m} \times 2\mu\text{m}$  level.<sup>14</sup>

In order to study the doping effect on GeH, we have successfully synthesized three doped GeH: P-GeH, Ga-GeH and A-GeH. In addition, we exfoliate the three types of doped GeH crystals into multilayers with measureable size ( $> 5\mu\text{m} \times 5\mu\text{m}$ ) onto  $\text{SiO}_2/\text{Si}$  substrates. The Polydimethylsiloxane (PDMS) is the optimized tape for exfoliation while lithium phenylacetylide cleaning process is added to optimize the cleaning effect. Besides, we also prove that all four types of GeH thin layers would be oxidized after one week exposure in the air based

on XPS and AFM measurements. The oxidizing rates would vary but the oxidization is limited on the surface layers. The oxidized parts can be dissolved by HCl aqueous solution while the fresh parts are stable in the HCl aqueous solution. Currently, we are working on four-probe and three-probe measurements to study the pure resistance of GeH materials, the carrier-concentration-dependent conductivity, the mobility of carriers and the identify the carriers.

## Chapter 2: Optimized Exfoliation of Multilayers

### 2.1 Exfoliation and Characterization

GeH is a van der Waals material and its crystal structure consists of single GeH sheets held mainly by weak van der Waals interactions. Therefore, single- and multi-atom-thick GeH layers can be isolated from bulk materials via the mechanical exfoliation, which has been demonstrated.<sup>14</sup> Three doped GeH crystals share similar interlayer interactions with pure GeH and can be exfoliated into single layers and multilayers on SiO<sub>2</sub>/Si substrates (**Figure 2.1**). Generally,  $1\text{cm} \times 1\text{cm}$  SiO<sub>2</sub>/Si substrates would be sonicated before exfoliation in acetone and isopropanol for 20 minutes, respectively, rinsed by deionized water and followed by 5-minute oxygen plasma treatment. The pre-exfoliation cleaning process is expected to remove both chemical residues and physical junks in order to create a clean and flat surface for getting flat exfoliated flakes. After exfoliation, the exfoliated samples are soaked in acetone and isopropanol for one hour, respectively, followed by deionized water rinsing and nitrogen flow drying.

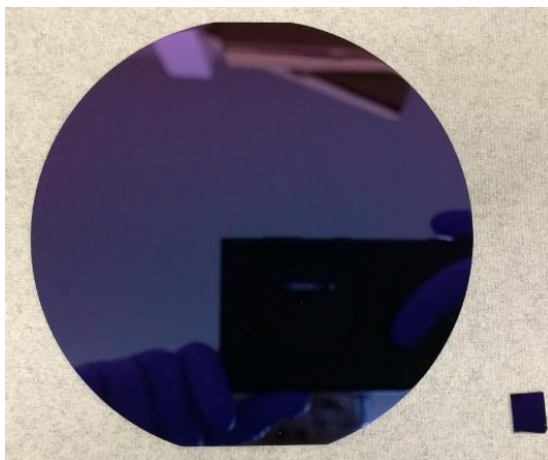


*Figure 2.1. Optical image of SiO<sub>2</sub>/Si wafer and applied substrate (right corner).*

The exfoliated flakes would be located via a microscope and evaluated by the atomic force microscopy (AFM). The combination of optical micrographs and AFM micrographs proves that the color of exfoliated thin sheets is related to its thickness. The previous work showed that single-layer sheets are light violet under the microscope (**Figure 2.2**).<sup>14</sup> When the thickness of

exfoliated sheets is lower than 10 nm, their color becomes deep blue (**Figure 2.3**). The optical color would be blue/cyan if the thickness range is from 13 nm to 27 nm (**Figure 2.4, 2.5a**). As the thickness of thin sheets continues to increase ( $< 45$  nm), the optical color would become green/yellow (**Figure 2.5b**). In addition, the optical micrograph of thin sheets also become chunky with an increasing thickness (**Figure 2.6**) and the uniformity of surface color means a flat surface (**Figure 2.5**). Atomic force microscopy (AFM) is a precise probe for analyzing the surface at nanoscale and its images (**Figure 2.2 – 2.6**) can evaluate the exfoliated flakes quantitatively to see if they are capable of making fabricating devices. Generally, the AFM probe (**Figure 2.7**) is oscillated at its fundamental resonance and the oscillation amplitude (the detector single) can be set to keep a constant distance between the probe and the analyzed surface so the output single offers information about thickness of flakes on the scanned surface.<sup>20</sup>

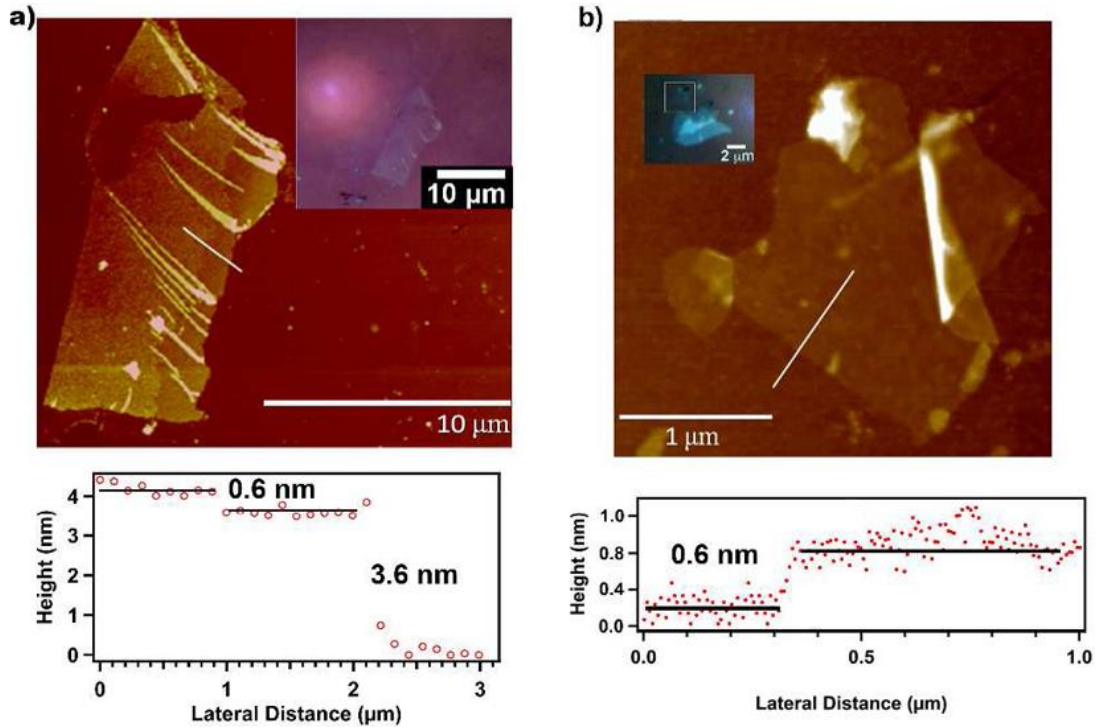


Figure 2.2. (a) AFM image (top), optical image (inset) and height profile of few-layer GeH flake on  $\text{SiO}_2/\text{Si}$ . (b) AFM image (top), optical image (inset) and height profile of single-atom-thick GeH flake.<sup>14</sup>

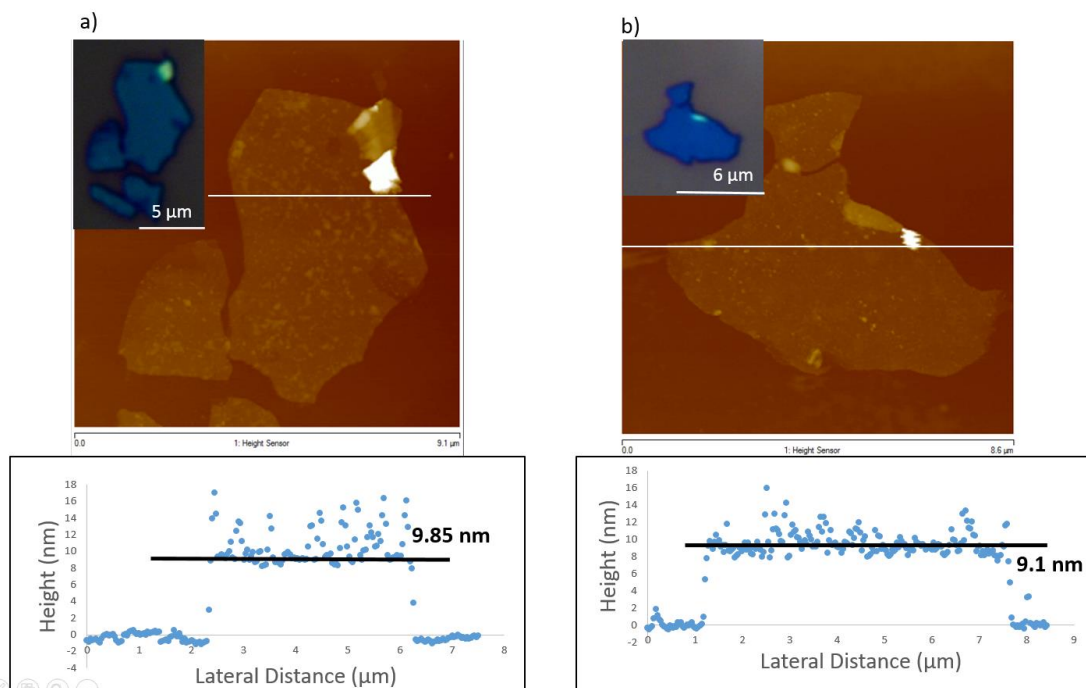


Figure 2.3. (a) AFM image (top), height profile (bottom), and optical micrograph (inset) of 9.85-nm-thick P-GeH sheet. (b) AFM image (top), height profile (bottom), and optical micrograph (inset) of 9.1-nm-thick P-GeH sheet.

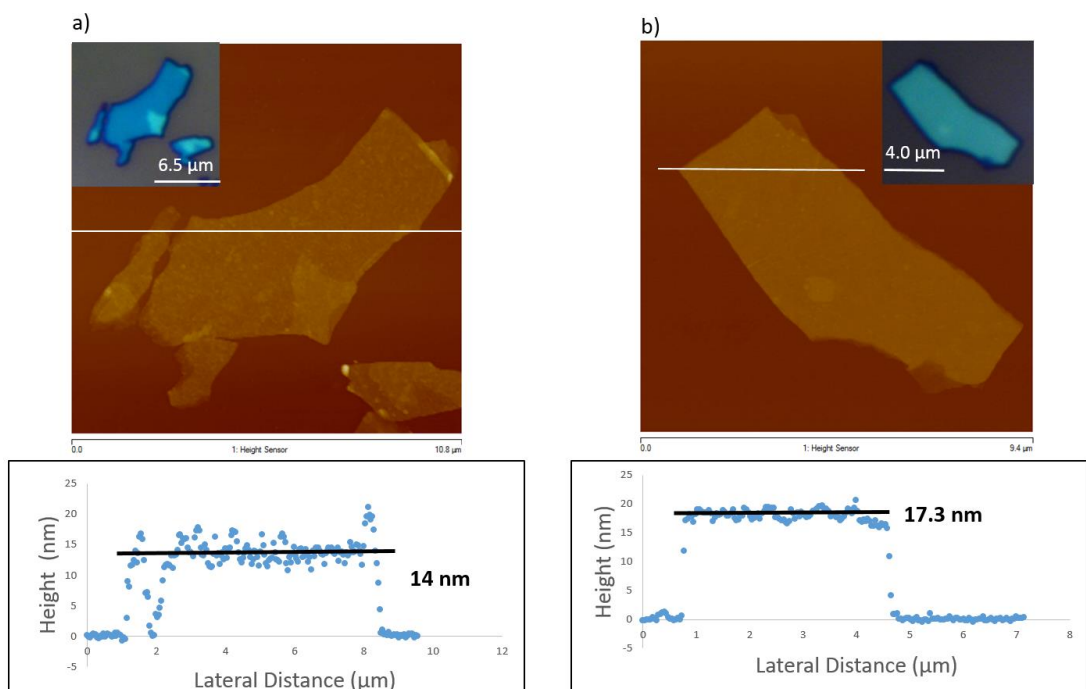


Figure 2.4. (a) AFM image (top), height profile (bottom), and optical micrograph (inset) of 14-nm-thick P-GeH sheet. (b) AFM image (top), height profile (bottom), and optical micrograph (inset) of 14.3-nm-thick P-GeH sheet.

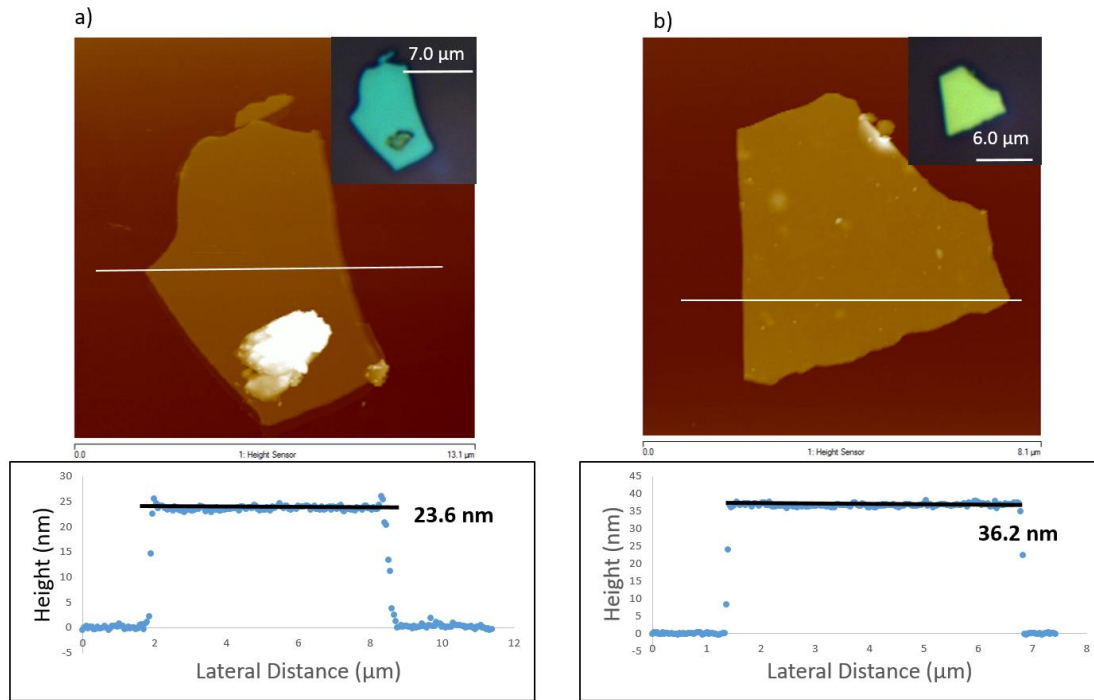


Figure 2.5. (a) AFM image (top), height profile (bottom), and optical micrograph (inset) of 23.6-nm-thick P-GeH sheet. (b) AFM image (top), height profile (bottom), and optical micrograph (inset) of 36.2-nm-thick Ga-GeH sheet.

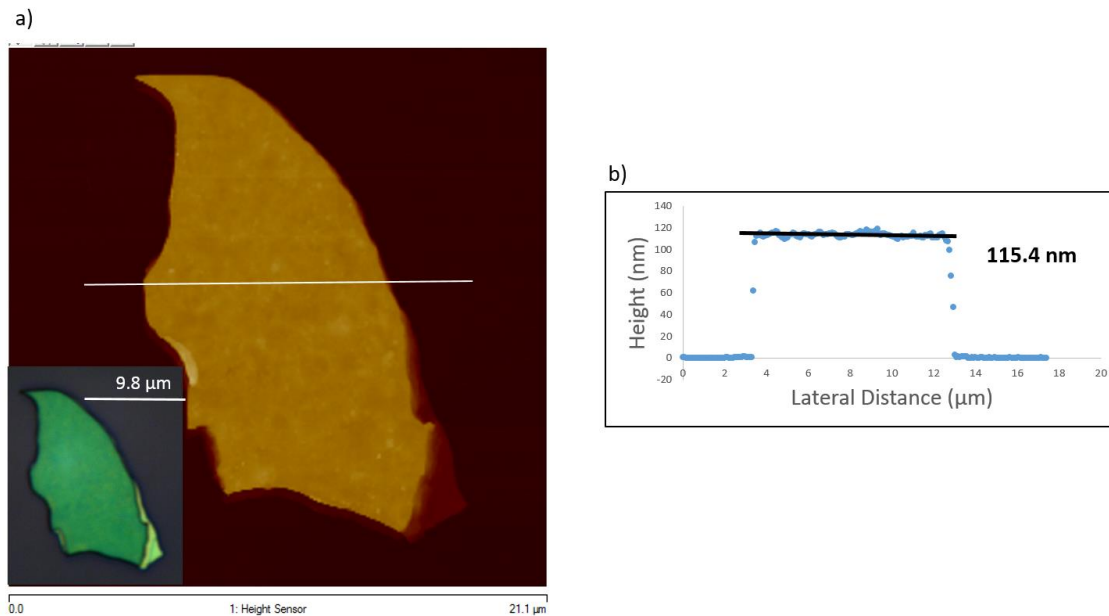


Figure 2.6. AFM image (top), height profile (bottom), and optical micrograph (inset) of 115.4-nm-thick GeH sheet.

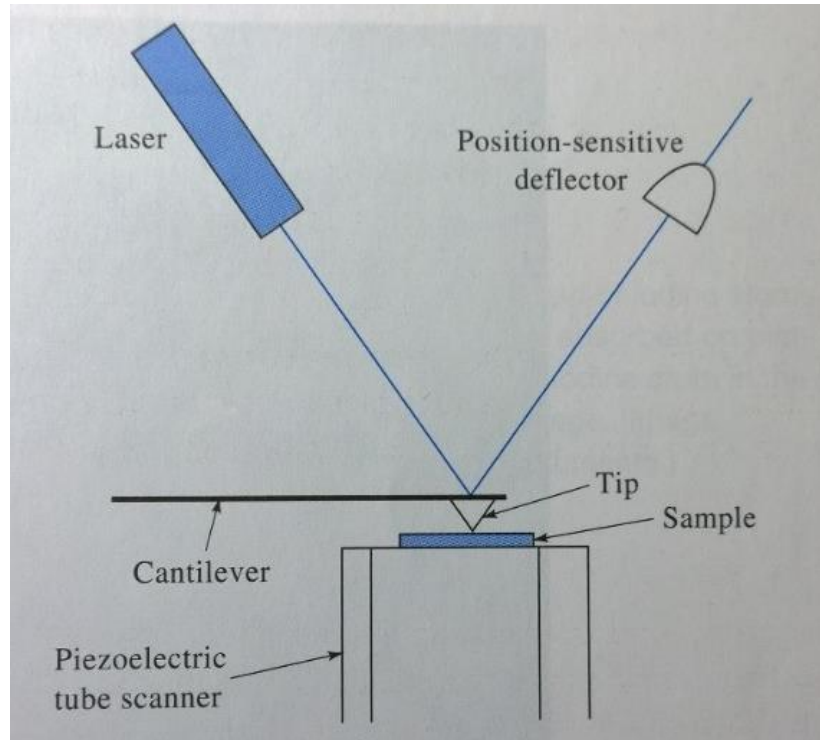
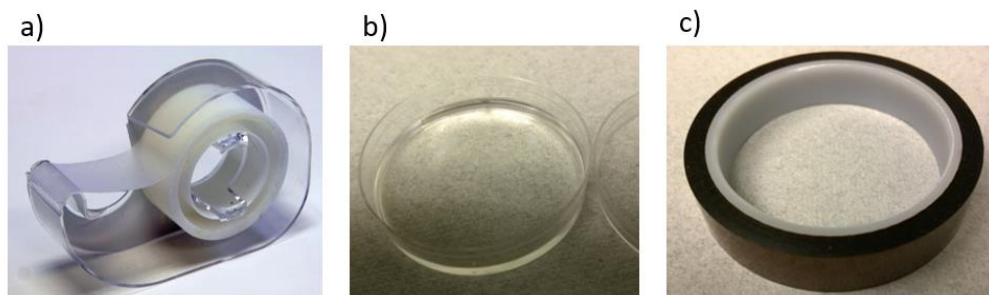


Figure 2.7. Diagrammatic sketch of atomic force microscopy (AFM) structure.<sup>20</sup>

## 2.2 Optimized Tape Choice for Exfoliation

As for exfoliation, choosing a suitable tape is important. Exfoliated flakes would finally be used to make fabricating devices for further studies such as optical and electronic properties. When preparing fabricating devices, flakes would be spin-coated with methyl methacrylate (MMA) first followed by poly (methyl methacrylate) (PMMA). After baking the spin-coated substrates for a period of time, the electron beam operation (E-beam) would be placed on the MMA-PMMA-covered surface in order to remove the residues on the thin sheets. Methyl isobutyl ketone (MIBK) and isopropanol are applied on the substrate surface as the developer to adhere the metal conductors. Finally, the fabricating device would be rinsed by acetone to remove MMA and PMMA. In order to characterize the electric properties, four-probe and three-probe measurements would be placed on the fabricating devices so the acceptable thin flakes should be at least  $5\ \mu\text{m} \times 5\ \mu\text{m}$ . A flat surface is also required or the metal conductors cannot

touch the flakes well, which can disrupt the electric property studies. Ideally, the exfoliated flake thickness should be  $\sim 5.5 \text{ \AA}$ , which is the thickness of single layers. However, the 1.53 eV band gap is not a unique property of GeH single-layer sheets because GeH multilayer sheets have a similar band gap.<sup>14</sup>



*Figure 2.8. (a) Optical image of scotch tape. (b) Optical image of polydimethylsiloxane (PDMS). (c) Optical image of kapton tape.*

We used scotch tape (**Figure 2.8a**), polydimethylsiloxane (PDMS) (**Figure 2.8b**), and kapton tape (**Figure 2.8c**) to exfoliate four types of GeH crystals onto the  $\text{SiO}_2/\text{Si}$  substrates. Kapton tape can produce flat and large enough flakes for fabricating devices (**Figure 2.5a**). However, the kapton-tape-exfoliated samples cannot be spin-coated uniformly because the tape residues are left on the surface and these residues can block the spin-coat process (**Figure 2.9a right four substrates**). In contrast, the scotch-tape-exfoliated samples can be spin-coated uniformly (**Figure 2.9a left four substrates**) although the exfoliated flake are not flat and the surface is covered by residues (**Figure 2.9b**). In previous work, the single-layer GeH sheet was firstly exfoliated by PDMS which is made by mixing silicone elastomer base and silicone elastomer curing agent together by the mass ratio of 10:1. Distinct from previous two tapes, PDMS is slightly stick but very clean without aging disruption and flakes exfoliated by PMDS are also flat and measurable (**Figure 2.9c**). Therefore, PDMS is the optimized tape choice among tapes we have investigated.



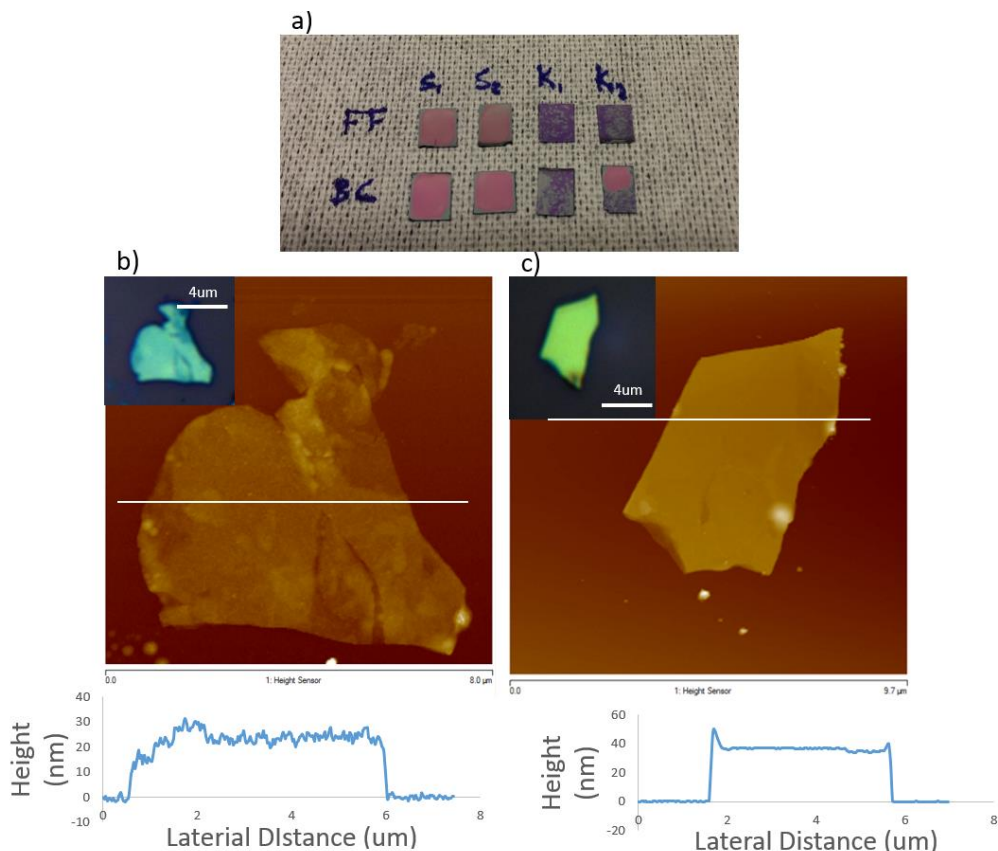


Figure 2.9. (a) Optical image of spin-coat comparison test sample. The left 4 substrates were exfoliated by the scotch tape while the right 4 were exfoliated by kapton tape. (b) AFM image (top), height profile (bottom), and optical micrograph (inset) of a scotch tape exfoliated As-GeH sample. (c) AFM image (top), height profile (bottom), and optical micrograph (inset) of a PDMS exfoliated Ga-GeH sample.

### 2.3 Optimized Cleaning Process

However, the PDMS-exfoliated substrates (**Figure 2.10a**) usually have some bright spots on the surface including the PDMS residues which cannot dissolve in acetone and isopropanol. Lithium phenylacetylide is expected to be capable of removing PDMS residues (**Figure 2.10b**). In this case, lithium phenylacetylide acts as a nucleophile while PDMS acts as an electrophile (**Figure 2.11**). In PDMS, O is more electronegative than Si so O is partially negative charged while Si bears a partially positive charge. In lithium phenylacetylide, the carbon-carbon triple grabs one electron from lithium so the  $C\equiv C^-$  can attack the Si – O bond from PDMS and finally dissolve PDMS. Circles in figure 2.10a mark the bright spots disappeared in figure 2.10b while the height profile shows that the flake surface is not etched after 90 min in lithium

phenylacetylide, too. Therefore, lithium phenylacetylide can remove PDMS residues and is safe to GeH flakes.

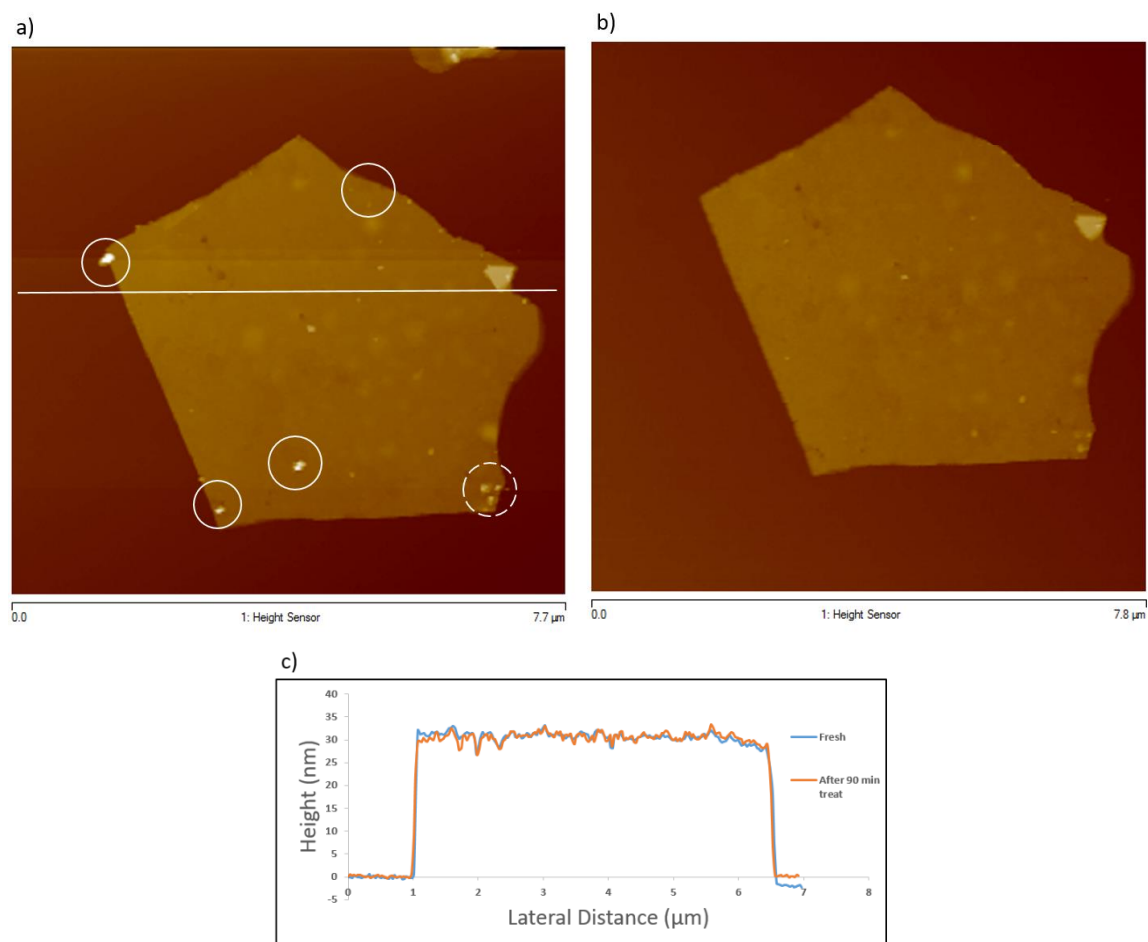


Figure 2.10. (a) Fresh exfoliated Ga-GeH flake. (b) The same flake after 90 min lithium phenylacetylide treatment. (c) Height profile of (a) and (b).

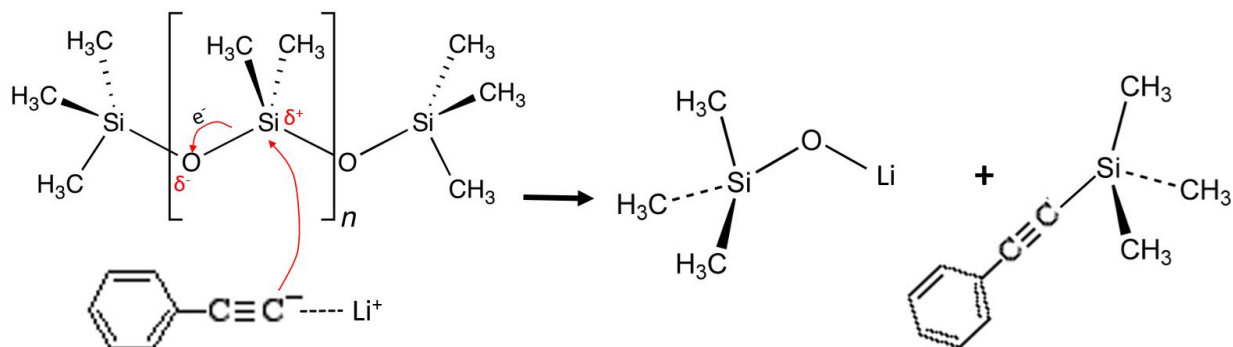


Figure 2.11. Schematic illustration of PDMS dissolving in lithium phenylacetylide.

### Chapter 3: Synthesis and Characterization of Germanane and its Derivatives

Recently, Goldberger's group has developed gram-scale crystallites of hydrogen-terminated germanium. Generally, GeH is synthesized by the topotactic deintercalation of  $\beta$ - $\text{CaGe}_2$  in the concentrated HCl aqueous solution for one week and the reaction system is at  $-40^\circ\text{C}$  (Figure 3.1).  $\beta$ - $\text{CaGe}_2$  crystals are prepared firstly by grinding Ca and GeH together at stoichiometric ratios and being sealed in the quartz tube followed by annealing to  $950^\circ\text{C}$  -  $1050^\circ\text{C}$  and then cooling down to the room temperature in 2 ~ 10 days (Figure 3.1b). After one week in the concentrated HCl solution, the product is rinsed by distilled water as well as methanol to get pure germanane (Figure 3.1 c). The purity of both  $\beta$ - $\text{CaGe}_2$  and GeH is demonstrated via X-ray diffraction (Figure 3.1de), respectively.<sup>14</sup>

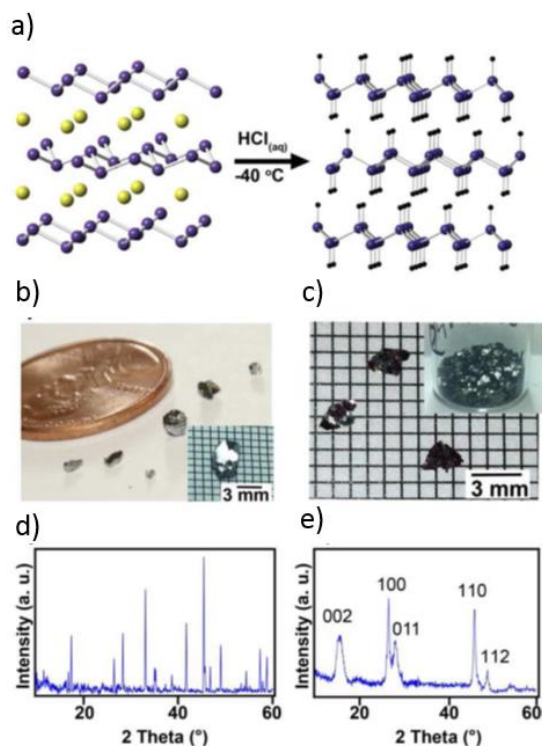


Figure 3.1 (a) Schematic illustration of the GeH preparation. (b) Optical image of  $\text{CaGe}_2$  crystal. (c) Optical image of GeH crystal. (d) XRD diagram of (b). (e) XRD diagram of GeH.<sup>14</sup>

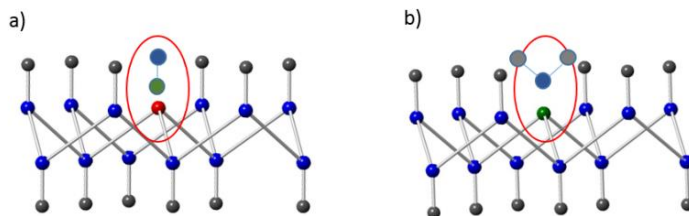


Figure 3.2. Schematic diagrams of (a) As-GeH and P-GeH and (b) Ga-GeH.

As for studying the doping effect on germanane, we have developed three doped germanane: phosphorus-doped germanane (P-GeH), gallium-doped germanane (Ga-GeH) and arsenic-doped germanane (As-GeH). P-GeH and As-GeH (**Figure 3.2a**) are n-type semiconductor materials because both P and As have one more electron on the outer shells than Ge. Ga-GeH (**Figure 3.2b**) is a p-type semiconductor material because its outer shell has one electron less than Ge. The syntheses of all the three doped GeH are quite similar to it of pure GeH. As for the synthesis of As-GeH,  $\beta$ -CaGe<sub>2</sub> is replaced by CaGeAs which shares a similar solid state synthesis process with  $\beta$ -CaGe<sub>2</sub>. Then CaGeAs crystals react with concentrated HCl solution at -40°C for one week to get As-GeH. Ga-GeH and P-GeH are prepared by the topotactic deintercalation of CaGeGa and CaGeP in the concentrated HCl at -40°C for one week, respectively. The purity of As-GeH and Ga-GeH has been demonstrated by X-ray diffraction spectroscopy, respectively (**Figure 3.3a**). In addition, XRD diagrams also show that the crystal structures of As-GeH and Ga-GeH are similar to GeH. P-GeH is very similar to As-GeH so its crystal structure should be similar to pure germanane, too.

Fourier transform infrared spectroscopy (FTIR) (**Figure 3.3b**) and Raman spectroscopy (**Figure 3.3c**) were also applied to determine the crystal structure of Ga-GeH and As-GeH. In the transmission mode, Ga-GeH and As-GeH have Ge-H stretch peaks at  $\sim 2000 \text{ cm}^{-1}$  and Ge-H wagging peaks at  $\sim 476 \text{ cm}^{-1}$ . In addition, a Ge-H<sub>2</sub> bending peak is also observed at  $\sim 822 \text{ cm}^{-1}$  in

both Ga-GeH and As-GeH. In Raman spectra, there are vibrational peaks at 230 nm ( $A_1$  mode) and 303 nm ( $E_2$  mode), respectively. Therefore, doping Ga and As do not change the crystal structure of GeH.

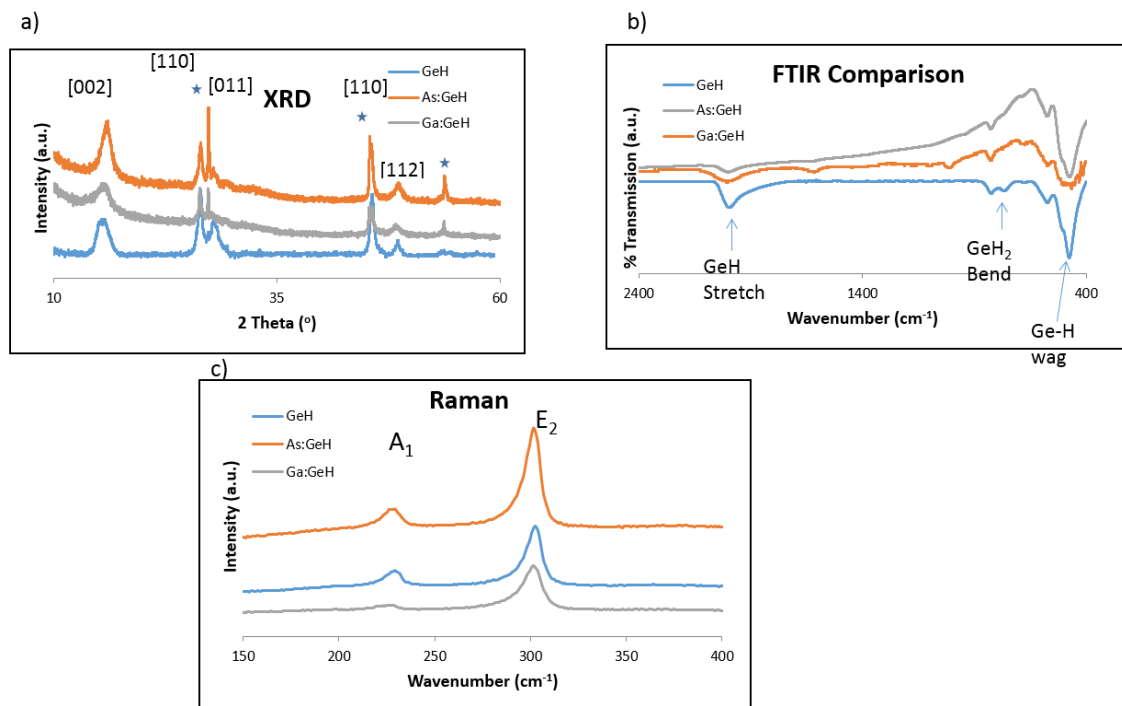


Figure 3.3. (a) XRD spectra (b) FTIR spectra and (c) Raman spectra of Ga-GeH, As-GeH and GeH.

## Chapter 4: Stability Studies

### 4.1 Air-Stability (XPS)

The previous work has proven that the hydrogen-terminated germanium materials can be oxidized slowly in the ambient atmosphere but the oxidization is bounded to the top layer (about 0.5 nm) while the bulk part is still resistant to the air.<sup>14</sup> Sensors, transistors and LED are commonly exposed to the air and the air-stability of GeH promises its potential applications on these areas.

Doped GeH materials have a higher carrier concentration so the conductivity should be better than pure germanane. Therefore, we set a series of time-dependent XPS measurements to investigate the air-stability properties of doped GeH. In this case, Ga-GeH (**Figure 4.1a**) and As-GeH (**Figure 4.1b**) were analyzed. As for Ga-GeH, the sample was scanned immediately followed by being exposed to the ambient atmosphere and scanned after 1 day, 4 days and 8 days, respectively. After one day in the air, the 2p Ge<sup>+</sup> peak at 1214.6 eV has a shoulder peak at 1220 nm which is Ge<sup>2+/3+</sup> and the intensity of this shoulder peak is close to the Ge<sup>+</sup> peak after 8 days in the air (**Figure 4.1a**).

The-time dependent XPS investment of As-GeH is very similar to Ga-GeH. In the 2p Ge XPS spectra, the Ge<sup>+</sup> peak has an intensive shoulder peak after 8 days (**Figure 4.1b**). In addition, the intensity of 2p Ge<sup>2+/3+</sup> peak is very close to the 2p Ge<sup>+</sup> peak after 8 days in the air for both As-GeH and Ga-GeH. As for pure GeH, however, the Ge<sup>2+/3+</sup> peak is still much less intense than the Ge<sup>+</sup> peak after 5 months in the air (**Figure 4.2**). XPS is a sensitive method of identifying the oxidization state of elements on the surface, the peak intensity is related to the quantity of an

elements. In this case, the hypothesis is that the doped GeH would be oxidized more easily than the pure GeH.

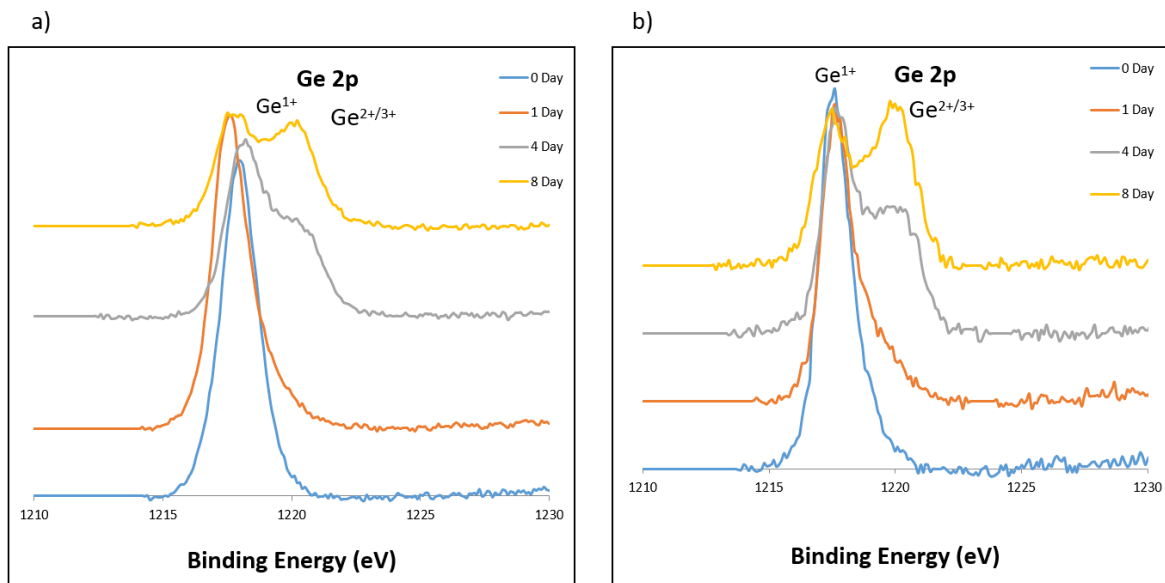


Figure 4.1. XPS spectrum of the Ge 2p peak for (a) Ga-GeH and (b) As-GeH.

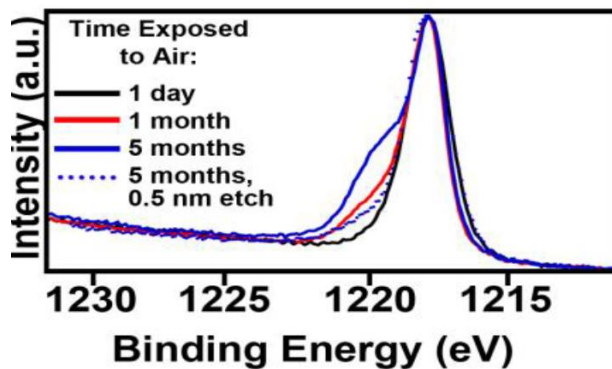


Figure 4.2. Time-dependent XPS spectra of GeH after exposure to the air for a period of time.<sup>14</sup>

#### 4.2 Air-Stability (AFM)

A time-dependent AFM study was placed to the air-stability studies of doped GeH. After one week exposure to the air (**Figure 4.3b**), there is no obvious changes on the thickness compared with the fresh flake (**Figure 4.3a**). After 30 seconds in 1 M HCl aqueous solution, this air-exposed Ga-GeH flake is etched by  $\sim 4$  nm (**Figure 4.3c**). In contrast, the fresh Ga-GeH flake

is etched little ( $\sim 1.5$  nm) after 30 seconds in 1 M HCl aqueous solution (**Figure 4.3f**). The only difference between an air-exposed flake and a fresh one is the length of oxidizing period.

Considering XPS spectra have showed that Ga-GeH would be oxidized in the air, oxidized Ga-GeH layers are dissolved by HCl aqueous solution.

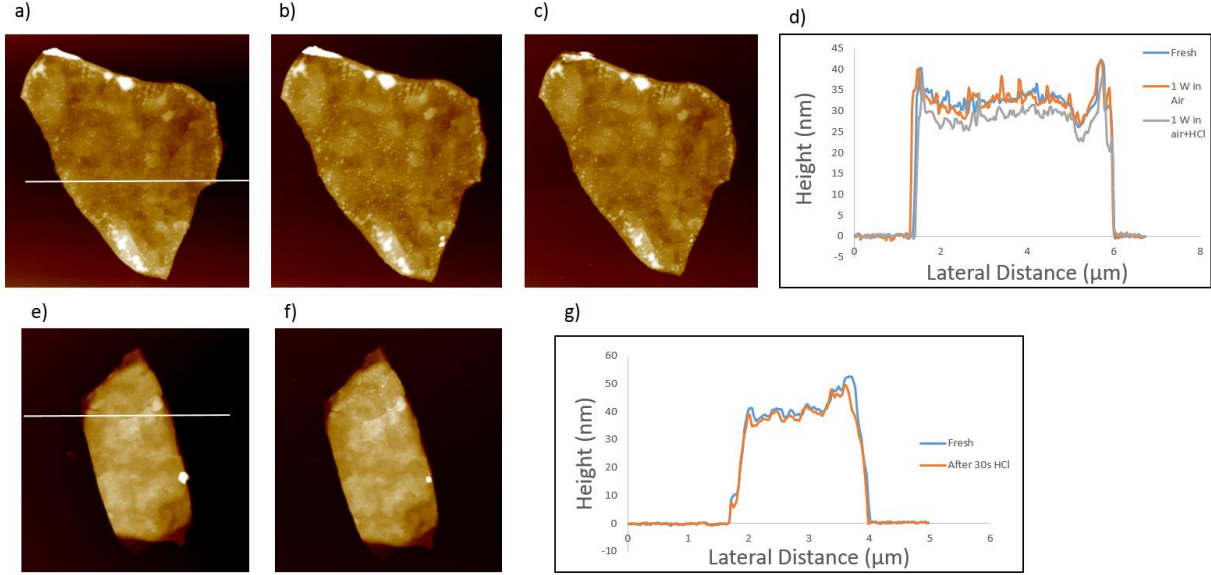


Figure 4.3. (a) AFM image of a fresh Ga-GeH flake. (b) AFM image of (a) after one week in air. (c) AFM image of (b) after 30 seconds 1 M HCl treat. (d) Height profile of (a), (b) and (c). (e) AFM of another fresh Ga-GeH flake. (f) AFM of (e) after 30 seconds in 1 M HCl. (g) Height profile of (e) and (f).

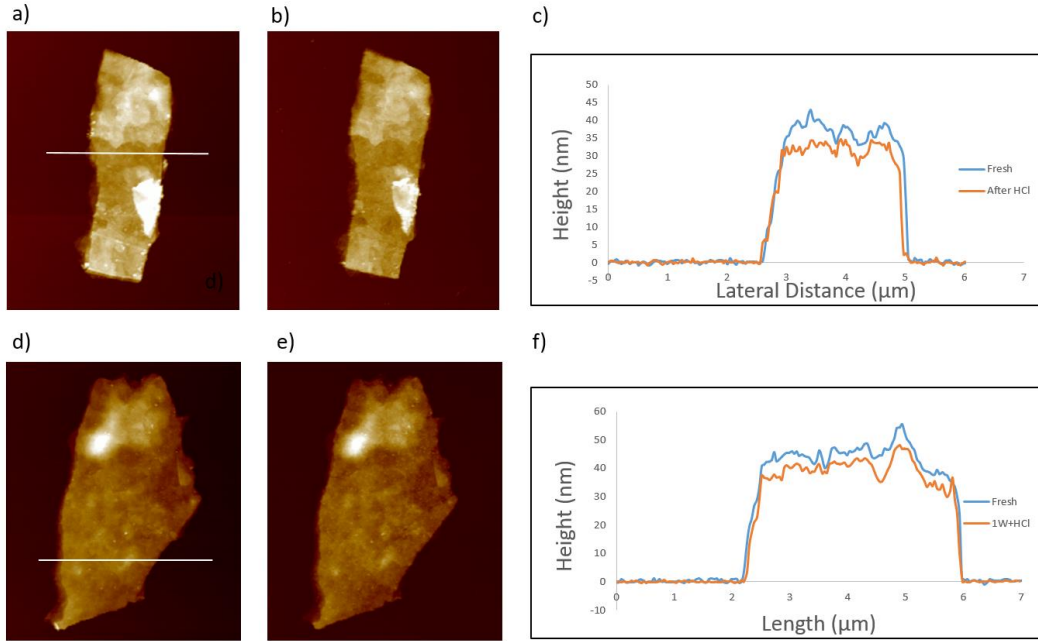


Figure 4.4 a) AFM image of a fresh As-GeH flake. (b) AFM image of (a) after 30 seconds in 1 M HCl. (c) Height profile of (a) and (b). (d) AFM of another fresh As-GeH flake. (e) AFM of (d) after one week exposure in the air followed by 30 seconds in 1 M HCl. (f) Height profile of (d) and (e).



In last section, XPS data have demonstrated that As-GeH and GeH can also be oxidized. We did the same 30 second 1 M HCl solution test on As-GeH, P-GeH and GeH, respectively, as what we did on Ga-GeH. The fresh As-GeH flake (**Figure 4.4a**) is etched by  $\sim 5$  nm in 1 M HCl aqueous solution according to the height profile of the oxidized flake (**Figure 4.4c**). The oxidized flake is etched by  $\sim 5$  nm after 30s in 1M HCl solution (**Figure 4.4e**). As for P-GeH, the one-week-air-exposure flake would be etched by 1 M HCl by  $\sim 7$  nm in 30 seconds compared with  $\sim 6$  nm etched thickness of a fresh P-GeH flake (**Figure 4.5**). Pure germanane is relatively stable: the fresh one can only be etched by  $\sim 0.3$  nm after HCl treatment (**Figure 4.6b**); the flake would be etched by  $\sim 4$  nm (**Figure 4.6e**) after one week in the ambient atmosphere followed by the same HCl treatment.

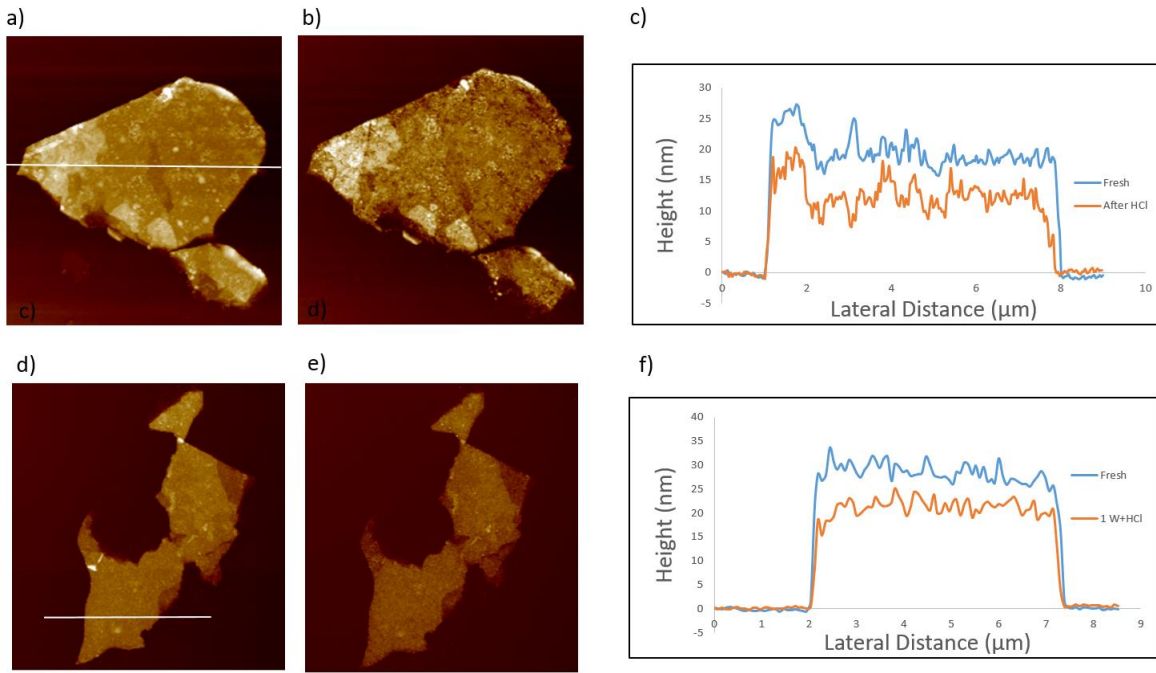


Figure 4.5. a) AFM image of a fresh P-GeH flake. (b) AFM image of (a) after 30 seconds 1 M HCl treatment. (c) Height profile of (a) and (b). (d) AFM of another fresh P-GeH flake. (e) AFM of (d) after one week exposure in the air followed by 30 seconds in 1 M HCl. (f) Height profile of (d) and (e).

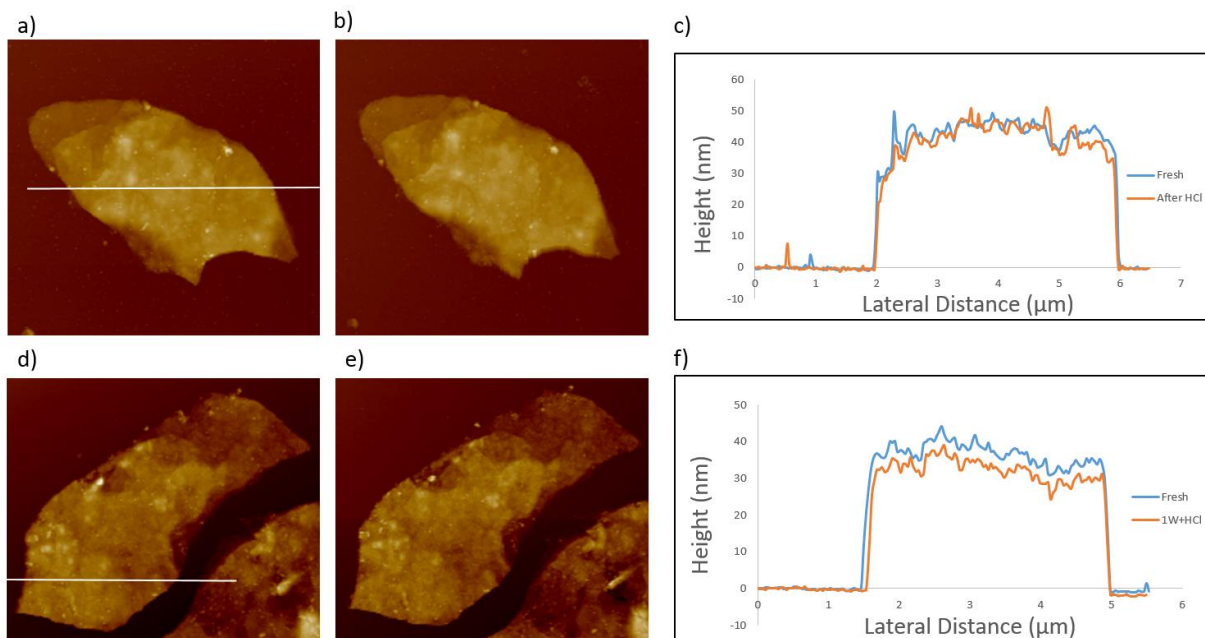


Figure 4.6. (a) AFM image of a fresh GeH flake. (b) AFM image of (a) after 30s 1 M HCl treatment. (c) Height profile of (a) and (b). (d) AFM of another fresh GeH flake. (e) AFM of (d) after one week in the air followed by 30 seconds in 1 M HCl. (f) Height profile of (d) and (e).

It is clear that the etching phenomenon is independent of the GeH types because all 4 types of oxidized GeH flakes would be etched by 4 nm ~ 6 nm in 1 M HCl aqueous solution. In contrast, the etching rates on fresh flakes vary from each other. Therefore, the oxidizing rate can be determined based on the etching effect on fresh flakes and four types of germanane materials have the following oxidizing rate order:

$$\text{P-GeH} \sim \text{As-GeH} > \text{Ga-GeH} > \text{GeH}.$$

### 4.3 HCl-Stability

As mentioned previously, GeH is prepared by the topotactic deintercalation of  $\text{CaGe}_2$  in concentrated HCl aqueous solution at low temperature for at least one week. Another three doped GeH crystals are prepared in similar processes as GeH. In addition, all the 4 types of GeH would be oxidized in the ambient atmosphere and the oxidized layers can dissolve in 1 M HCl aqueous solution. Therefore we placed a 30-second-HCl-treatment versus 1200-second-HCl treatment test (**Figure 4.7**) to test if the HCl solution can etch the fresh layers.

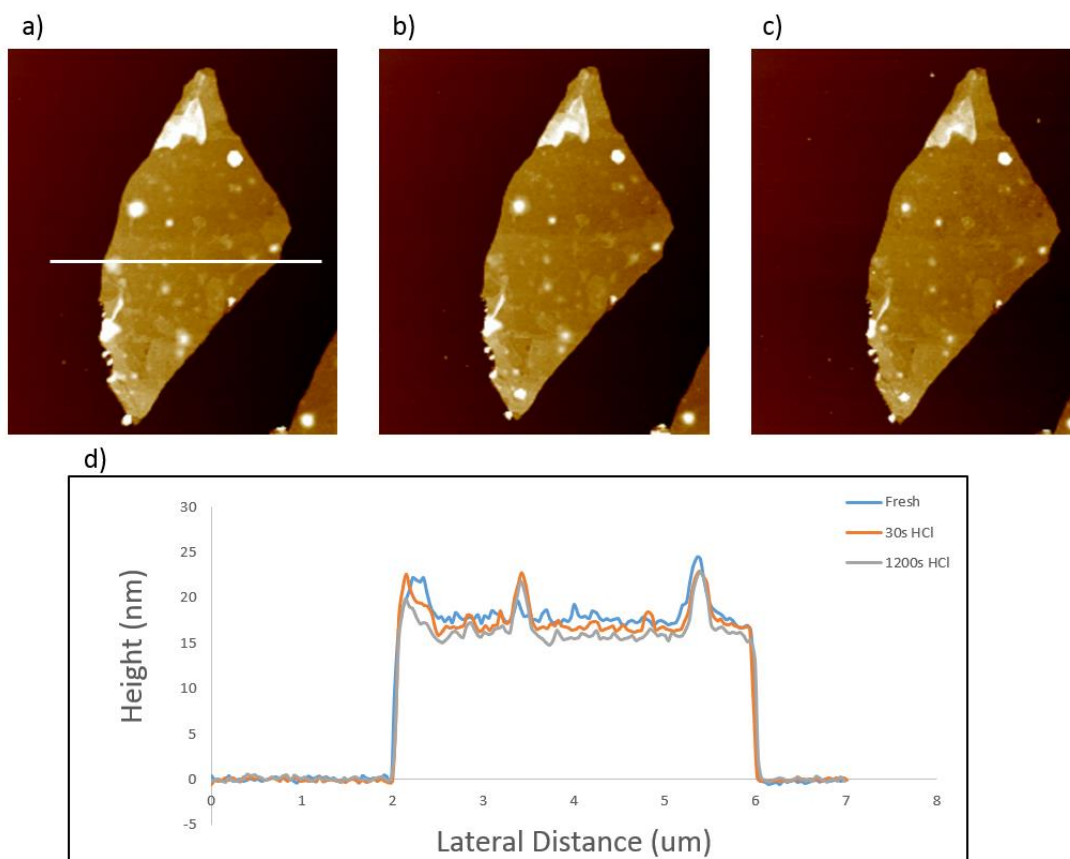


Figure 4.7. (a) AFM image of fresh-exfoliated Ga-GeH. (b) AFM image of (a) after 30 seconds 1 M HCl treatment. (c) AFM image of (b) after 1200 seconds 1 M HCl treatment. (d) Height profile of (a), (b) and (c).

We firstly scan a fresh-exfoliated Ga-GeH flakes under AFM. Then we place a 30-second-1-M-HCl-treatment on the same flake and scan this flake under AFM. Next, we would place a 1200-second-1-M-HCl-treatment on the same flake and scan under AFM again. Compared with the fresh AFM image (**Figure 4.7a**), the 30-second-1-M-HCl-treatment can etch the flake by  $\sim 0.8$  nm (**Figure 4.7b**). The flake is etched by  $\sim 1.0$  nm after 1200-second-1-M-HCl-treatment (**Figure 4.7c**) compared with the flake after 30-second-HCl-treatment. Generally, two AFM measurements on the same object would be slightly different because the applied attractive potentials between the AFM tips and the substrate are slightly different in each two trials.<sup>21</sup> Therefore, the etching effect is a time-independent phenomenon once the HCl treatment

is longer than 30 seconds. In this case, we set a hypothesis that the GeH materials are resistant to the HCl aqueous solution but the oxidized layers would be dissolved by the HCl solution.

## Chapter 5: Further Work

2D materials have properties distinct from their parent materials because of the reduced dimensionality. The Group IV graphane analogues are a new class of 2D materials that show exceptional promise in a wide range of optical and electronic applications. Although we set a route for getting measureable GeH multilayers instead of single-layer materials, multilayer materials still have many potential applications such as batteries and supercapacitors.<sup>19</sup> We currently are measuring the electric properties on different types of germanane materials. The exfoliated flakes would be applied to make fabricating devices in the clean room and 4-probe measurements as well as 3-probe measurements would be placed on the fabricating devices. The 4-probe measurement is designed to eliminate the disturbance from the applied conducting materials and is capable of demonstrating the resistance of germanane materials directly. The 3-probe measurement is applied to measure the carrier-concentration-dependent conductivity, the mobility of carriers and identify the carrier (holes or electrons).

Generally, germanane materials are resistant to the air while the surface parts can still be oxidized. In addition, precise electric measurements require a clean surface to minimize unknown contributions. A 30 second UV-ozone cleaning process followed by 30 seconds 1 M HCl treatment is applied because the ozone plasma cleaning can remove chemical residues and oxidizes flakes slightly compared with the oxygen plasma cleaning (**Figure 5**). Besides, we have developed doped GeH materials with doping concentration range 1% to 3% and in the soon future, we plan to develop doped GeH crystals with doping concentrations as high as possible to make GeH 2D materials more conductive because the conductance is proportional to the number of electron carriers.

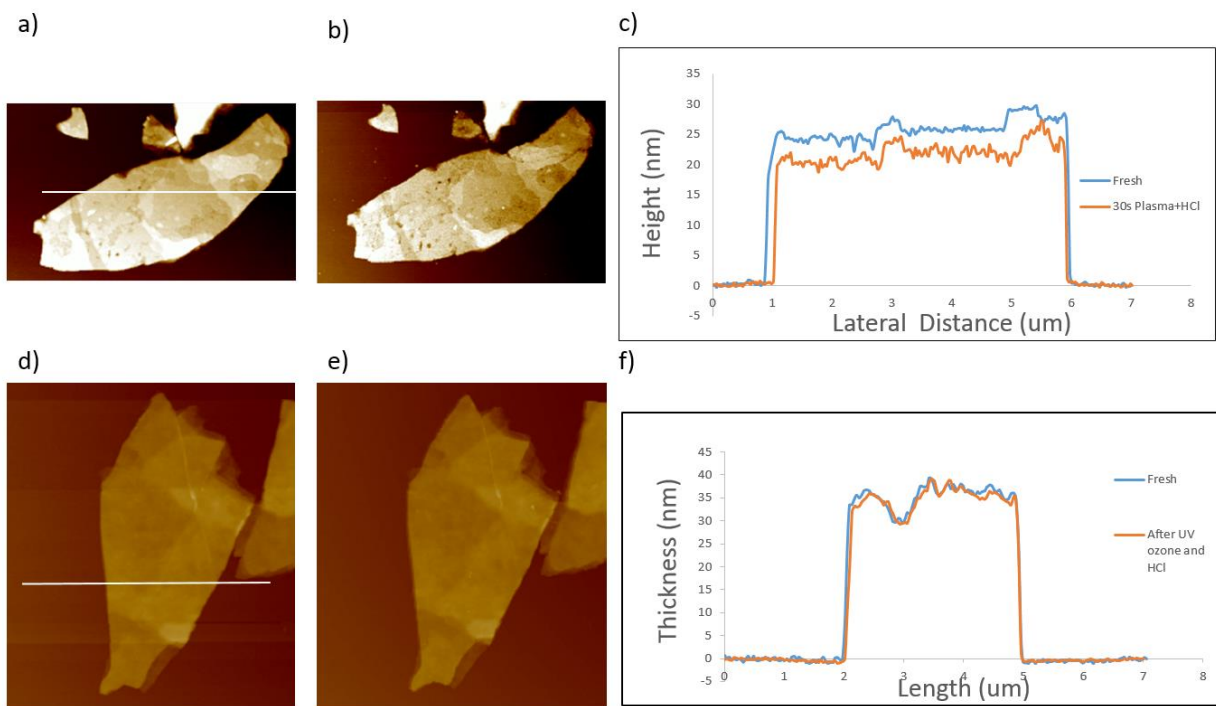


Figure 5. (a) AFM image of fresh Ga-GeH flake. (b) AFM of (a) after 30 second oxygen plasma followed by 30 seconds 1 M HCl treatment. (c) Height profile of (a) and (b). (d) AFM of fresh Ga-GeH flake. (e) AFM of (d) after 30 seconds UV-ozone process followed by 30 seconds 1 M HCl. (f) Height profile of (d) and (e).

## Conclusion

In summary, we have synthesized gram-scale crystallites of gallium-doped, arsenic-doped, and phosphorus-doped hydrogen-terminated germanium and demonstrated that all the three materials can be exfoliated into measureable multilayers on the  $\text{SiO}_2/\text{Si}$  substrates, which would be used to make fabricating devices for the optical and electrical property studies. Besides, we have proven the cleaning effect of lithium phenylacetylide on the polydimethylsiloxane residues. We have also characterized the oxidization-resistance of 4 types of exfoliated GeH, which is an important prerequisite for practical applications, and demonstrated that the oxidized layers can be dissolved by HCl aqueous solution, which essentially supports our synthesis procedure of GeH and its derivatives. Besides, the etching effect on different oxidized GeH flakes is quite similar: the etch height is 4~6 nm for all the four GeH materials although they have different oxidizing rate. In this case, we hypothesize that the pure GeH materials are resistant to the HCl aqueous solution while the oxidized layers are not; the oxidization is limited on the surface while the left layers are resistant to the air. Thus, the stability of GeH and its three derivatives meets the prerequisite of potential applications.

## References:

1. Novoselov, K. S.; Geim, A. K.; Morozov, S. V.; Jiang, D.; Katsnelson, M. I.; Grigorieva, I. V.; Dubonos, S. V.; Firsov, A. A. Two-Dimensional Gas of Massless Dirac Fermions in Graphene *Nature* **2005**, *438*, 197-200.
2. Novoselov, K. S.; Geim, A. K.; Morozov, S. V.; Jiang, D.; Zhang, Y.; Dubonos, S. V.; Grigorieva, I. V.; Firsov, A. A. Electric Field Effect in Atomically Thin Carbon Films *Science* **2004**, *306*, 666-69.
3. Fowler, J. D.; Allen, M. J.; Tung, V. C.; Yang, Y.; Kaner, R. B.; Weiller, B. H. Practical Chemical Sensors from Chemically Derived Graphene *ACS Nano* **2009**, *3*, 301-6.
4. Liang, Y.; Li, Y.; Wang, H.; Zhou, J.; Wang, J.; Regier, T.; Dai, H. Co<sub>3</sub>O<sub>4</sub> Nanocrystals on Graphene as a Synergistic Catalyst for Oxygen Reduction Reaction *Nat. Mater.* **2011**, *10*, 780-86.
5. Williams, G.; Seger, B.; Kamat, P. V. TiO<sub>2</sub>-Graphene Nanocomposites. UV-Assisted Photocatalytic Reduction of Graphene Oxide *ACS Nano* **2008**, *2*, 1487-91.
6. Lee, C.; Yan, H.; Brus, L. E.; Heinz, T. F.; Hone, J.; Ryu, S. Anomalous Lattice Vibrations of Single- and Few-Layer MoS<sub>2</sub> *ACS Nano* **2010**, *4*, 2695-700.
7. Mak, K. F.; Lee, C.; Hone, J.; Shan, J.; Heinz, T. F. Atomically Thin MoS<sub>2</sub>: A New Direct-Gap Semiconductor *Phys. Rev. Lett.* **2010**, *105*, 136805.
8. Radisavljevic, B.; Radenovic, A.; Brivio, J.; Giacometti, V.; Kis, A. Single-layer MoS<sub>2</sub> Transistors *Nat. Nano.* **2011**, *6*, 147-50.
9. Long, J. R.; McCarty, L. S.; Holm, R. H. Solid Route to Molecular Clusters: Access to the Solution Chemistry of [Re<sub>6</sub>Q<sub>8</sub>]<sup>2+</sup> (Q=S, Se) Core-Containing Clusters via Dimensional Reduction. *J. Am. Chem. Soc.* **1996**, *118*, 4603-4616.



10. Kagan, C. R.; Mitzi, D. B.; Dimitrakopoulos, C. D. Organic-Inorganic Hybrid Materials as Semiconducting Channels in Thin-Film Field-Effect Transistors. *Science*. **1999**, 286, 945–947.
11. Huang, X.; Li, J.; Fu, H. The First Covalent Organic-Inorganic Networks of Hybrid Chalcogenides: Structures That May Lead to a New Type of Quantum Wells. *J. Am. Chem. Soc.* **2000**, 122, 8789–8790.
12. Mitzi, D. B. Solution Processing of Chalcogenide Semiconductors via Dimensional Reduction. *Adv. Mater.* **2009**, 21, 3141–3158.
13. Huang, X.; Roushan, M.; Emge, T. J.; Bi, W.; Thiagarajan, S.; Cheng, J.-H.; Yang, R.; Li, J. Flexible Hybrid Semiconductors with Low Thermal Conductivity: The Role of Organic Diamines. *Angew. Chem., Int. Ed.* **2009**, 48, 7871–7874.
14. Bianco, E.; Butler, S.; Jiang, S. S.; Restrepo, O. D.; Windl, W.; Goldberger, J. E. Stability and Exfoliation of Germanane: A Germanium Graphane Analogue. *ACS Nano*. **2013**, 7, 4414-21.
15. Elias, D. C.; Nair, R. R.; Mohiuddin, T. M. G.; Morozov, S. V.; Blake, P.; Halsall, M. P.; Ferrari, A. C.; Boukhvalov, D. W.; Katsnelson, M. I.; Geim, A. K.; Novoselov, K. S. Control of Graphene's Properties by Reversible Hydrogenation: Evidence for Graphane *Science* **2009**, 323, 610-13.
16. Lomeda, J. R.; Doyle, C. D.; Kosynkin, D. V.; Hwang, W.-F.; Tour, J. M. Diazonium Functionalization of Surfactant-Wrapped Chemically Converted Graphene Sheets *J. Am. Chem. Soc.* **2008**, 130, 16201-06.
17. Becerril, H. A.; Mao, J.; Liu, Z.; Stoltenberg, R. M.; Bao, Z.; Chen, Y. Evaluation of Solution-Processed Reduced Graphene Oxide Films as Transparent Conductors *ACS Nano* **2008**, 2, 463-70.

18. Vogg, G.; Brandt, M. S.; Stutzmann, M. Polygermyne\_A. Prototype System for Layered Germanium Polymers. *Adv.Mater.* **2000**, *12*, 1278–1281.
19. Butler, S. Z.; Hollen, S. M.; Cao, L.; Cui, Y.; Gupta, J. A.; Gutierrez, H. R.; Heinz, T. F.; Hong, S.; Huang, J.; Ismach, A. F.; Johnston-Halperin, E.; Kuno, M.; Plashnitsa, V. V.; Robinson, R. D.; Ruoff, R. S; Salahuddin, S.; Shan, J.; Shi, L.; Spencer, M. G.; Terrones, M.; Windl, W.; Goldberger, J. E. Progress, challenges, and opportunities in two-dimensional materials beyond graphene. *ACS nano*. **2013**, *7*, 2898-2926.
20. Skong, D. A.; Holler, F. J.; Crouch, S. R. *Principles of Instrumental Analysis, 6<sup>th</sup> Edition*; Thomson Brooks/Cole: Belmont, CA, 2007, 589-623.
21. Nemes-Incze, P.; Osvath, Z.; Kamaras, K.; Biro, L. P. Anomalies in Thickness Measurements of Graphene and Few Layer Graphite Crystals by Tapping Mode Atomic Force Microscopy. *Carbon*. **2008**, *46*, 1435–1442.